Atomic-scale observation of polarization switching in epitaxial ferroelectric thin films

D. L. Marasco, A. Kazimirov, M. J. Bedzyk,[a] and T.-L. Lee
Department of Materials Science, Northwestern University, Evanston, Illinois 60208 and Materials Science Division, Argonne National Laboratory, Argonne, Illinois 60439

S. K. Streiffer, O. Auciello, and G.-R. Bai
Materials Science Division, Argonne National Laboratory, Argonne, Illinois 60439

(Received 3 May 2001; accepted for publication 22 May 2001)

The thin-film x-ray standing wave (XSW) technique is used for an atomic-scale study of polarization switching in ferroelectric $Pb(Zr_{0.3}Ti_{0.7})O_3$ (PZT)/electrode heterostructures grown on $SrTiO_3(001)$. The XSW is selectively generated in the PZT by the interference between the incident x-ray wave and the weak (001) Bragg diffracted wave from the film. The XSW excites a fluorescence signal from the Pb ions in the PZT film, that is used to determine their subangström displacements after polarization switching has occurred. This experimental method yields unique information on the underlying atomic configurations for different polarization domain states. © *2001 American Institute of Physics.* [DOI: 10.1063/1.1385349]

Interest in the synthesis and characterization of perovskite-based ferroelectric thin films has recently increased because of their utilization in microelectronic devices,[1] including nonvolatile ferroelectric random access memories (FeRAMs). The two main ferroelectric materials already being used in low-density devices are $PbZr_xTi_{1-x}O_3$ (PZT) and $SrBi_2Ta_2O_9$.[1] In particular, PZT thin films possess excellent characteristics, such as large remanent polarization and relatively low synthesis temperatures,[2] that are required for continued development of many applications.

However, further research is necessary to better understand the fundamental ferroelectric behavior of these materials in thin-film form. Extensive characterization of critical phenomena, including polarization switching, fatigue, and imprint, have been performed using electrical[3] and piezo-response[4] methods. However, these techniques do not provide unambiguous insight into the atomistic processes underlying the polarization switching response. New approaches for directly studying the atomic-scale structural changes in switched ferroelectric films are required. In this vein, the acentric polarity of *as-grown* ferroelectric films has recently been studied using synchrotron x-ray scattering[5] and x-ray standing wave (XSW)[6] methods. This polarity is equivalent to the polarization vector direction (for the simple case of a single domain sample), and thus can be used to investigate lattice structural processes that are involved in polarization dynamics. Since x-rays can easily penetrate a top electrode, these methods are also particularly well suited for application to realistic ferroelectric-electrode heterostructures. In this letter, we discuss studies focused on establishing a correlation between polarization switching and atomic-scale structural changes of the ferroelectric lattice.

In a traditional XSW experiment, the XSW is generated by a strong Bragg reflection from a bulk perfect single crystal.[7] The outgoing diffracted plane wave interferes with the incident plane wave and forms a standing wave field. This standing wave field has the same periodicity as the diffraction planes. As the crystal is advanced in angle through the arcsec wide ''total reflection,'' the antinodes of the standing wave field shift from a location halfway between the diffraction planes to a position coincident with the planes. This inward shift of the antinodes causes an angle-dependent modulation in an atom's fluorescence signal that can be used to determine that atom's lattice position(s). Ignoring extinction, the normalized fluorescence yield from a sublattice of a particular atomic species can be expressed as[8]

$$Y_H^j(\theta) = 1 + R(\theta) + 2\sqrt{R(\theta)}|S_H^j| e^{-M_H^j - W_H^j} \cos[v(\theta) - \varphi_H^j], \tag{1}$$

where $R(\theta)$ is the reflectivity, $v(\theta)$ is the relative phase of the diffracted wave, $|S_H^j|$ and φ_H^j are the modulus and phase of the geometrical structure factor for the jth sublattice, and $e^{-M_H^j}$ and $e^{-W_H^j}$ are the thermal and static Debye–Waller factors, respectively.

As demonstrated recently,[6,9] x-ray standing wave fields can also be generated by weak Bragg diffraction from a single crystal thin film. Unlike the Bragg peak of a bulk reflection, a thin film Bragg peak has a much weaker reflectivity and much wider angular width. For thin films, the XSW-induced modulation in the fluorescence yield varies as $\sqrt{R}$ [Eq. (1)]. Based on kinematical diffraction theory[10] one can show that for a 20 nm PZT film the (001) Bragg peak reflectivity is ~0.1%. This should lead to modulation in the XSW fluorescence signal of ~3%. To observe this very small modulation, it is necessary to collect $\sim 1\times 10^6$ fluorescence counts at each angular step of the rocking curve. This can be readily achieved at a synchrotron source capable of generating a high-brightness x-ray beam.

In this study, the XSW is generated in an 20-nm-thick epitaxial PZT film that was grown[2] at 700 °C by metalorganic chemical vapor deposition, on an epitaxial 136-nm-thick $SrRuO_3$ layer sputter deposited at 680 °C,[11,12] onto a

[a]Electronic mail: bedzyk@northwestern.edu

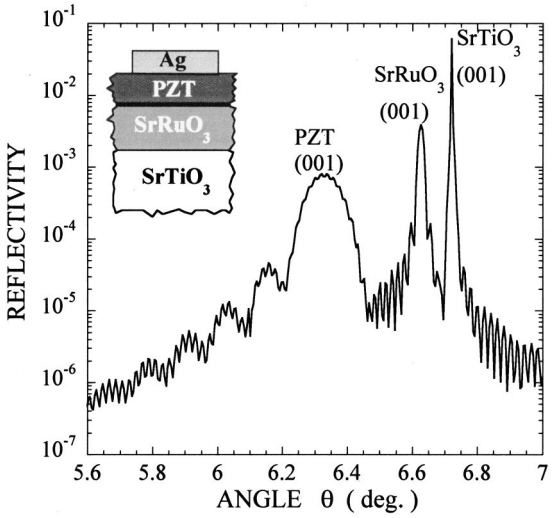

FIG. 1. Experimentally measured x-ray reflectivity of the PZT capacitor structure taken at $\lambda=0.914$ Å. The inset shows the layers within the heteroepitaxial structure: a $SrTiO_3$ (001) substrate, a 136-nm-thick $SrRuO_3$ bottom electrode, a 20-nm-thick PZT film, and a 30-nm-thick Ag top electrode. The angle positions for the three distinct (001) Bragg peaks mark off the three distinct c lattice constants of $SrTiO_3$, $SrRuO_3$, and PZT. The two patterns of oscillation are due to the thickness of the $SrRuO_3$ and PZT films, the smaller period oscillation belongs to the thicker film. The Ag top electrode has a polycrystalline structure and does not measurably contribute to the scattered intensity in this high-resolution scan.

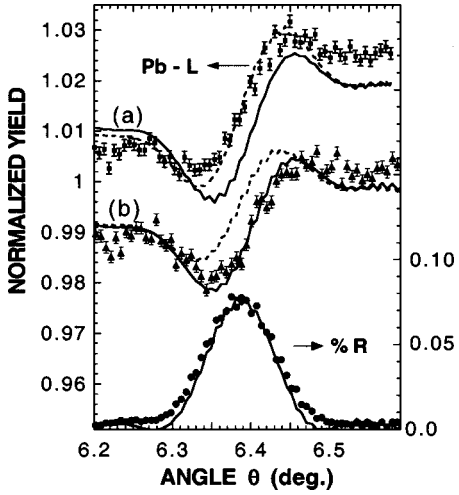

FIG. 2. Experimental XSW data measured from a 20-nm-thick PZT (001) film that had been polarized (a) down and (b) up at the completion of its hysterisos loop. The data consist of the angle θ dependence of the normalized Pb $L\alpha$ fluorescence yield and reflectivity in the vicinity of the PZT (001) reflection at an incident energy of 13.50 keV. The best fits for the up and down polarities are shown as solid and dashed lines, respectively. The yield data and theory curves for (a) were given a 0.02 vertical offset for purposes of clarity.

single crystal $SrTiO_3$ substrate. The substrate was miscut 1.9° from the (001) and 12° from the in-plane [010] directions in order to promote highly ordered growth of the orthorhombic $SrRuO_3$, which served as a bottom electrode. Polycrystalline Ag top electrodes 30 nm thick were electron beam evaporated through a shadow mask onto the surface of the continuous PZT film, thus defining capacitor structures. The bulk properties of the solid solution $Pb(Zr_{0.3}Ti_{0.7})O_3$ can be found in Ref. 13. At temperatures above the paraelectric/ferroelectric phase transition ($T_c^{\text{bulk}}\sim 425\,^{\circ}\text{C}$) PZT is macroscopically centric, with the Pb^{2+} ions at the cell corners, the Zr^{4+}/Ti^{4+} at the body-center position, and the O^{2-} at the face-center sites. When cooled below T_c, a structural transition to an acentric unit cell occurs, accompanied by elongation of the cell along the polarization direction. In the bulk ferroelectric state the Pb^{2+} and Zr^{4+}/Ti^{4+} sublattices are shifted from their centric positions in the unit cell relative to the O^{2-} planes by fractional displacements along the c axis. This generates a net polarization that can be switched by the application of an external electric field, corresponding to a reversal in the sign of the displacements for 180° switching. Here, we use the thin-film XSW method to examine the c-axis displacement of the Pb^{2+} sublattice in PZT thin-film capacitors after being poled ''up'' (or ''down'') by an externally applied field.

Figure 1 shows the x-ray reflectivity data taken at $\lambda=0.914$ Å through the (001) Bragg peaks of the PZT and $SrRuO_3$ layers, and the $SrTiO_3$ substrate. The scattering is modulated with two periodicities, corresponding to the thickness fringes of the PZT and $SrRuO_3$. The existence of these oscillations indicates that both the $SrRuO_3$ and PZT films have good structural coherence.[14]

The top electrode of a selected capacitor was then connected to the output voltage of a function generator, while the bottom electrode was held at ground. As the bias voltage was cycled, the current was measured in order to monitor the ferroelectric switching behavior. (Note that a positive voltage applied to the top electrode will cause the positive ions in the PZT lattice to shift downward, and therefore we refer to this state as polarized down.) Some capacitors showed hysteresis loops that were shifted off center in voltage, suggesting the existence of a ''hard'' and an ''easy'' state of polarization. This phenomenon is generally referred to as imprint.[15] For our particular capacitors, this imprint phenomenon may be due to the manner in which the PZT films grow on the $SrRuO_3$ bottom electrode layers and to the asymmetry in the heterostructure.

The XSW measurements were performed on a four-circle diffractometer at the DND-CAT 5-ID-C station of the Advanced Photon Source at Argonne National Laboratory. The x-ray undulator radiation was monochromatized to 13.50 keV by the beamline's Si (111) liquid nitrogen cooled double-crystal monochromator. The incident beam slits were set to produce an approximately 180-μm-wide by 240-μm-long x-ray footprint at the (001) Bragg angle. The beam was positioned on the desired 250-μm-diam capacitor by observing the Ag L fluorescence from the top electrodes. An energy dispersive solid-state detector was used to collect the x-ray fluorescence spectra, while a NaI scintillation detector recorded the x-ray reflected intensity. For the XSW measurement the Pb $L\alpha$ fluorescence was collected simultaneously with the reflectivity as the sample was rocked through the PZT (001) Bragg peak (see Fig. 2).

The fluorescence data were analyzed using an extension[16] of Takagi–Taupin dynamical diffraction theory[17] to calculate the total D-field intensity at various depths within the ferroelectric film. The simulation curves included in Fig. 2 were obtained by modeling the $SrTiO_3$ substrate as a centrosymmetric cubic crystal with a lattice spacing of 3.905 Å. The $SrRuO_3$ was treated as tetragonal crystal with an in-plane lattice constant matched to the substrate and an

out-of-plane lattice constant of 3.970 Å. The tetragonal PZT layer was modeled as having an out-of-plane lattice constant of $c=4.130$ Å. These c lattice constants were derived from the Bragg peaks in Fig. 1. The fractional sublattice displacements of the ions that give rise to the ferroelectric nature of the PZT were assumed to be the same as for bulk $PbTiO_3$. This is a reasonable approximation given the accuracy of the XSW measurement and taking into account the PZT cell distortion induced by epitaxial strain. This model was used to calculate the expected fluorescence yield and reflectivity for the polarized up and down cases for the PZT film. These two cases were fit to the data with the static Debye–Waller factor as a free parameter, using a chi-squared minimization algorithm.

Four capacitors were examined after being scanned through their $I-V$ hysteresis loops. Two devices were left in the down orientation and two in the up orientation. For the two capacitors that were left in the down orientation, the analysis of the XSW data is clear. The experimental data closely match the theory curves for a down polarized film rather than an up one. The static Debye–Waller factors were 0.67 for one of these down polarized ferroelectric capacitors and 0.84 for the other. The XSW data analysis for the latter case is shown in Fig. 2(a). For the two capacitors externally polarized in the up orientation, we found by XSW analysis that one of these capacitors is clearly in the up orientation, while the other fits down better than up, with Debye–Waller factors of 0.71 and 0.78, respectively. The XSW data analysis for the former case is shown in Fig. 2(b). While the ratio of the goodness-of-fit parameters between the best fits for the up and down cases was 2 for the other cases, the ratio for the last capacitor was 1.4.

The particular poled up capacitor that reversed its polarization during the period between poling and x-ray measurements can be explained by backswitching, and is in agreement with the electrical measurements that showed a preferred down orientation for that capacitor. This demonstrates that the XSW method can be used as a nondisturbing probe of the (dynamic) polarization state of a ferroelectric film, in contrast to electrical switching measurements, which by their nature tend to destroy the probed domain state. Furthermore, the information that is contained in the Debye–Waller factor is unique to this measurement, in that different Debye–Waller factors may yield additional insight into different domain configurations or mixtures that may be present in a sample.

In summary the x-ray standing wave method was used to probe the atomic-scale structure of electrically switched ferroelectric thin film/electrode heterostructures. The success of this type of measurement opens the door to more complex endeavors. For example, by combining the thin film x-ray standing wave method with x-ray microfocusing and *in situ* biasing, one could observe real-time switching with micron-scale lateral resolution. Therefore, not only can the static structure be studied with this method, but also can the dynamics of thin-film ferroelectric switching.

The authors thank C.-B. Eom and R. A. Rao of Duke University for growing the $SrRuO_3$ epitaxial layers and the DND-CAT staff for assistance at the beamline. This work was supported by the DoE under Contract Nos. W-31-109-ENG-38 to Argonne National Laboratory (ANL) and DE-F02-96ER45588 to Northwestern University (NU), by the NSF under Grant Nos. DMR-9973436 and DMR-0076097, and by the State of Illinois under Contract No. IBHE HECA NWU 96 to NU.

[1] O. Auciello, J. F. Scott, and R. Ramesh, Phys. Today **51**, 22 (1998).
[2] G.-R. Bai, I.-F. Tsu, A. Wang, C. M. Foster, C. E. Murray, and V. P. Dravid, Appl. Phys. Lett. **72**, 1572 (1998).
[3] See, for example, *Ferroelectric Thin Films: Synthesis and Basic Properties*, edited by C. A. P. Araujo, J. F. Scott, and G. W. Taylor (Gordon and Breach, New York, 1996).
[4] O. Auciello, A. Gruverman, H. Tokumoto, S. A. Prakash, S. Aggarwal, and R. Ramesh, MRS Bull. **23**, 33 (1998).
[5] C. Thompson, C. M. Foster, J. A. Eastman, and G. B. Stephenson, Appl. Phys. Lett. **71**, 3516 (1997).
[6] M. J. Bedzyk, A. Kazimirov, D. L. Marasco, T.-L. Lee, C. M. Foster, G.-R. Bai, P. F. Lyman, and D. T. Keane, Phys. Rev. B **61**, R7873 (2000).
[7] B. W. Batterman, Phys. Rev. Lett. **22**, 703 (1969).
[8] A. Kazimirov, M. Kovalchuk, and V. Kohn, Sov. Tech. Phys. Lett. **14**, 587 (1988).
[9] A. Kazimirov, T. Haage, L. Ortega, A. Stierle, F. Comin, and J. Zegenhagen, Solid State Commun. **104**, 347 (1997).
[10] R. W. James, *The Optical Principles of the Diffraction of X-rays* (Cornell University Press, Ithaca, NY, 1965).
[11] Q. Gan, R. A. Rao, and C. B. Eom, Appl. Phys. Lett. **70**, 1962 (1997).
[12] C. B. Eom, R. J. Cava, R. M. Fleming, J. M. Phillips, R. B. van Dover, J. H. Marshall, J. W. P. Hsu, J. J. Krajewski, and W. F. Peck, Jr., Science **258**, 1766 (1992).
[13] F. Jona and G. Shirane, *Ferroelectric Crystals* (Dover, New York, 1993), and references therein.
[14] For a detailed x-ray scattering analysis of a similar heterostructure, see C. Thompson, A. Munkholm, S. K. Streiffer, G. B. Stephenson, K. Ghosh, J. A. Eastman, O. Auciello, G.-R Bai, M. K Lee, and C. B. Eom, Appl. Phys. Lett. **78**, 3511 (2001).
[15] W. L. Warren, B. A. Tuttle, D. Dimos, G. E. Pike, H. N. Al-Shareef, R. Ramesh, and J. T. Evans, Jpn. J. Appl. Phys., Part 1 **35**, 1521 (1996).
[16] T. L. Lee and M. J. Bedzyk (unpublished).
[17] S. Takagi, Acta Crystallogr. **15**, 1311 (1962); J. Phys. Soc. Jpn. **26**, 1239 (1969); D. Taupin, Bull. Soc. Fr. Mineral. Cristallogr. **87**, 469 (1964).